

# Ubiquitous non-local entanglement with Majorana bound states

Alessandro Romito<sup>1</sup> and Yuval Gefen<sup>2</sup>

<sup>1</sup>*Department of Physics, Lancaster University, Lancaster LA1 4YB, United Kingdom*

<sup>2</sup>*Department of Condensed Matter Physics, The Weizmann Institute of Science, Rehovot 76100, Israel*

Entanglement in quantum mechanics contradicts local realism, and is a manifestation of quantum non-locality. Its presence can be detected through the violation of Bell, or CHSH inequalities. Paradigmatic quantum systems provide examples of both, non-entangled and entangled states. Here we consider a minimal complexity setup consisting of 6 Majorana bound states. We find that *any* allowed state in the degenerate Majorana space is non-locally entangled. We show how to measure (with available techniques) the CHSH-violating correlations, using either intermediate strength or weak measurement protocols.

**Introduction** Majorana zero-modes are a particular class of states, hosting non-Abelian quasi-particles that reflect the topologically non-trivial character of the underlying system. Over less than a decade Majorana bound states (MBS) have crossed the line from mathematically intriguing constructs, solid state manifestations of Majorana's original particles [1–3], to experimentally realizable entities [4–6]. Being a class of non-Abelian anyons [7, 8], MBS offer a paradigm for fault-tolerant information processing [9]. Following initial experiments [10–15], we are now at the stage where specific platforms for engineering and manipulating Majoranas [16–18] are being implemented. It is broadly felt that implementations of topological states of matter for quantum information processing should rely, first, on thorough understanding of Majorana quantum states. Interestingly, a unique property of MBS is that they may constitute a manifestation of quantum non-locality. Indirect observable signatures emerging from non-local MBS (albeit not a proof of their non-locality) have been studied earlier in setups based on mesoscopic superconductors [19–21], or coupled Majorana bound states [22, 23].

Non-locality is an indispensable pillar of quantum mechanics. For a system made of at least two particles non-locality is a manifestation of quantum entanglement between spatially distinct degrees of freedom. For paradigmatic systems, an apt example being two spin-1/2 particles, it is possible to construct both entangled (e.g. a singlet) and non-entangled, i.e. product (e.g. triplet-1) states [24]. Quantum non-locality is quantified by Bell's inequality [25], or, in a manner that is more conducive to experimental testing [26, 27], by the violation of the Clauser, Horne, Shimony and Holt (CHSH) inequality [28].

The focus of the present study is the direct observability of entanglement of quantum states constructed of Majorana bound states. We identify a system of minimal complexity (minimal number of MBS). For that system: (i) we show that *any* allowed quantum state made up of a superposition of MBS is non-locally entangled; (ii) we then demonstrate how such entanglement can be detected within technologically feasible measurement plat-

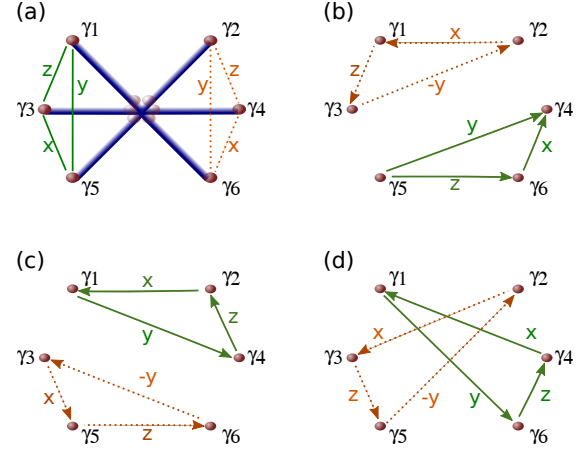


FIG. 1. (a): Multi-terminal junction of topological superconducting wires (blue) hosting Majorana bound states at their ends (red dots). The Majorana end-states at the junction (fading red) are gapped up and the six Majorana end-states (solid red dots)  $\gamma_1, \dots, \gamma_6$  constitute the low energy excitations of the system. A left detector (not shown) measures the operators indicated by solid (green) arrows, which are labeled by the corresponding spin algebra operators, e.g.  $Z = -i\gamma_1\gamma_2$  playing the role of  $\sigma_z$ . Dashed (orange) arrows define the operators measured by the right detector. Panels (a-d) show different possible partitionings into left and right sectors with the corresponding operators. CHSH inequalities are necessarily violated in at least one of the partitionings in (a-d).

forms; (iii) finally, we show how our entanglement detection protocol can be realized within weak measurement operations.

**Model** Our system consists of a multi-terminal junction made up of an even number of one-dimensional topological superconductors (branches), depicted in Fig. 1(a). They all have a common end point at the center. Such experimentally available segments are made of semiconductor wires with spin orbit coupling proximatized by s-wave superconductors [10–12, 14]. Alternatively, they are made of magnetic impurity chains embedded in superconductors [13]. Each segment,  $\alpha \in \{1, \dots, 2N\}$ , of this setup consists of a 1-d spinless p-wave superconductor characterized by a bulk excitation energy gap,  $\Delta_\alpha$ ,

and by zero-energy MBS at the end points,  $\gamma_\alpha, \gamma'_\alpha$ , localized at the wire's boundaries. The dynamics of these MBS is underlined by the algebra  $\{\gamma_\alpha, \gamma_\beta\} = 2\delta_{\alpha,\beta}$ ,  $\{\gamma_\alpha, \gamma'_\beta\} = 0$ . The wire Hamiltonian at energies well below the gap is given by  $H_\alpha = \epsilon_\alpha \gamma_\alpha \gamma'_\alpha$ , where  $\epsilon_\alpha \sim e^{-l_\alpha/\xi_\alpha}$  is exponentially small with the wire's length,  $l_\alpha$ . The latter is larger than the superconductor coherence length [3–5]  $\xi_\alpha \propto 1/\Delta_\alpha$ . We also assume  $\epsilon_\alpha = 0$ , which is a valid assumption as long as the duration of the measurement protocol is not too long. At the junction, the Josephson coupling between each pair of branches,  $\alpha, \beta$  results in a low energy coupling between the corresponding Majorana end-states. This is described by the Hamiltonian [3, 29]  $H_T = \sum_{\alpha,\beta} t_{\alpha,\beta} \gamma'_\alpha \gamma'_\beta$ . Generically, the tunnel coupling at the junction pairs up the  $2N$  Majorana end-states,  $\gamma'_1, \dots, \gamma'_{2N}$ , to finite energy states with energies  $\sim \min\{t_{\alpha,\beta}\}$ . These states are then projected out of the degenerate ground-state space. This leaves us with the Majorana states  $\{\gamma_\alpha\}$  that are far from the junction (see Fig. 1(a)). These represent the remaining zero energy degrees of freedom. They span a  $2^N$  degenerate ground state. The Majorana subspace does not accommodate a well-defined number of fermions: it may exchange pairs of fermions with the underlying superconductor. It follows that the parity of the Majorana system,  $\mathcal{P} = i \prod_{j=1}^{2N} \gamma_j$ , is a good quantum number, hence the degenerate ground-state space consists of two subspaces, each of a definite parity. Without loss of generality, we may restrict ourselves, in the low-energy space, to states in the  $2^{N-1}$ -dimensional odd subspace. We will study a minimal complexity setup consisting of  $2N = 6$  MBS.

The Majorana end-states,  $\gamma_1, \dots, \gamma_{2N}$ , can be partitioned into two different sets, left ( $L$ ), and right ( $R$ ); each of which is to be probed by a separate external detector. The detectors can be tuned to measure any combination of pairs of Majorana products. Physically this is a measurement of the occupancy of certain Dirac fermions degrees of freedom, constructed from the Majorana degrees of freedom. Details of the measurement procedure are discussed below. An example to be utilized below is depicted in Fig. 1(a), where the  $L$ -set consists of  $\gamma_1, \gamma_3, \gamma_5$ , and the coupled detector can measure any operator of the form

$$\hat{O}_L = -i(\cos \theta_L \gamma_1 \gamma_3 + \sin \theta_L \cos \phi_L \gamma_3 \gamma_5 + \sin \theta_L \sin \phi_L \gamma_5 \gamma_1). \quad (1)$$

Note that the expectation values of the measured observables are bounded,  $-1 \leq \langle O_L \rangle \leq 1$  (the eigenvalues of the bilinear Majorana products are  $\pm 1$ ). Genuine quantum correlations underlying a state can be identified through the expectation values of correlated measurements. Specifically, a state that can be described within a local hidden variable theory (a.k.a. local realism), satisfies the CHSH inequality [28]

$$\mathcal{C} \equiv |\langle \hat{O}_L \hat{O}_R \rangle - \langle \hat{O}_L \hat{O}'_R \rangle| + |\langle \hat{O}'_L \hat{O}_R \rangle + \langle \hat{O}'_L \hat{O}'_R \rangle| \leq 2, \quad (2)$$

where  $\hat{O}_L, \hat{O}'_L$  and  $\hat{O}_R, \hat{O}'_R$  are pairs of spatially separable sets of observables. For quantum non-locally entangled states, it is instead possible to choose the operators such that [30]  $2 < \mathcal{C} \leq 2\sqrt{2}$ , hence providing evidence of genuine quantum correlations. Eq.(2) is an equivalent formulation of Bell's inequality [25, 28], which, relying only on averaged correlation outputs, can be tested directly by averaging over repeated measurements, including weak measurements.

Entangled states that violate Bell's and CHSH inequalities are common in quantum mechanics. Alternatively, one may construct product states which are non-entangled. The novel aspect of our work is that we show that in the degenerate space spanned by Majorana end states, *any* state is non-locally entangled. In other words, one can always find (at least) one partitioning of the MBS into two spatially separable sets, where the CHSH inequality is violated. Loosely speaking, for any state in the degenerate ground-space it is possible to design non-local measurements that reveal intrinsic non-locality.

To begin with, we realize that establishing the CHSH relations requires measurement of non-commuting observables for each of the separated-in-space parts of the system, *i.e.* the  $L$  and  $R$  sets. For observables bilinear in the elementary MBS (cf. Eq. (1)), this requires a minimum of three Majorana operators for each set. The minimal complexity setup appropriate for our purpose is therefore a multi-terminal junction consisting of six branches (6 MBS) (cf. Fig. 1(a)). We consider a generic state of the 4-degenerate odd parity ground-manifold. Following the labeling of the Majoranas in Fig.1(a), such a state is parametrized as

$$|\psi\rangle = A d_{1,3}^\dagger d_{4,2}^\dagger d_{5,6}^\dagger |0\rangle + B d_{1,3}^\dagger |0\rangle + C d_{4,2}^\dagger |0\rangle - D d_{5,6}^\dagger |0\rangle, \quad (3)$$

where  $|A|^2 + |B|^2 + |C|^2 + |D|^2 = 1$ . Here we have introduced the fermionic degrees of freedom,  $d_{1,3}^\dagger = (\gamma_1 + i\gamma_3)/2$ ,  $d_{4,2}^\dagger = (\gamma_4 + i\gamma_2)/2$ ,  $d_{5,6}^\dagger = (\gamma_5 + i\gamma_6)/2$ , and the state  $|0\rangle$  is defined by  $d_{1,3}|0\rangle = 0$ ,  $d_{5,6}|0\rangle = 0$ ,  $d_{4,2}|0\rangle = 0$ . Throughout our analysis we will switch between Fock space states, spin-1/2 states, and Majorana notation.

Consider the partitioning depicted in Fig. 1(a):  $\gamma_1, \gamma_3, \gamma_5$  constitute the ( $L$ ) set;  $\gamma_2, \gamma_4, \gamma_6$  – the ( $R$ ) set. The operators  $\hat{Z}_L \equiv -i\gamma_1\gamma_3$ ,  $\hat{X}_L \equiv -i\gamma_3\gamma_5$ ,  $\hat{Y}_L \equiv -i\gamma_5\gamma_1$  satisfy the Pauli matrix algebra,  $\sigma_z = \hat{Z}_L$ ,  $\sigma_x = \hat{X}_L$ ,  $\sigma_y = \hat{Y}_L$ . It follows that measurement of an operator of the form of Eq. (1) can be mapped onto the measurement of  $\hat{O}_L = \hat{\sigma} \cdot \mathbf{n}$ , where  $\hat{\sigma} = 2\hat{\mathbf{S}}$  is a spin-1/2 operator and  $\mathbf{n} \equiv (\sin \theta_L \cos \phi_L, \sin \theta_L \sin \phi_L, \cos \theta_L)$ . Analogously,  $\hat{Z}_R \equiv -i\gamma_4\gamma_2$ ,  $\hat{Y}_R \equiv i\gamma_2\gamma_6$ ,  $\hat{X}_R \equiv -i\gamma_6\gamma_4$  can be identified with Pauli operators of the right set. In such spin-1/2 language the state  $|\psi\rangle$  reads  $|\psi\rangle = A |\uparrow_L \uparrow_R\rangle + B |\uparrow_L \downarrow_R\rangle + C |\downarrow_L \uparrow_R\rangle + D |\downarrow_L \downarrow_R\rangle$ , where  $|\uparrow_i\rangle, |\downarrow_i\rangle$  are the eigenstates of  $\hat{Z}_i$  ( $i = L, R$ ). The maximal value of

the CHSH correlation  $\mathcal{C}$  in Eq. 2 is given by

$$\mathcal{C}_{135|246} = 2\sqrt{1 + 4|AD - BC|^2}, \quad (4)$$

where the subscript indicates the partitioning in which the measurement is performed. For any state,  $2 \leq \mathcal{C}_{135|246} \leq 2\sqrt{2}$ , and  $\mathcal{C}_{135|246} \neq 2$  signals non-local correlations, which happens unless  $AD - BC = 0$ . Operationally, this means that, if  $AD - BC \neq 0$  one can select the coefficients  $\theta_L, \theta_R, \phi_L, \phi_R$  to construct a proper set of operators that violate the CHSH inequality.

Though a given state might not violate the CHSH inequality with measurements within the specific  $L$  and  $R$  sets, it can still lead to a violation of the CHSH inequality with a different partitioning of the MBS. The new partitioning will be non-local in the old  $L$  and  $R$  sets. For example, a different partitioning consisting of the sets  $\tilde{L}$  and  $\tilde{R}$  is depicted in Fig. 1(b), where the left detector is connected to  $\gamma_5, \gamma_6, \gamma_4$  while  $\gamma_1, \gamma_3, \gamma_2$  are connected to the right detector. In this case we define the operators  $\hat{Z}_{\tilde{L}} \equiv -i\gamma_5\gamma_6, \hat{X}_{\tilde{L}} \equiv -i\gamma_6\gamma_4, \hat{Y}_{\tilde{L}} \equiv -i\gamma_4\gamma_5$ , and  $\hat{Z}_{\tilde{R}} \equiv -i\gamma_1\gamma_3, \hat{Y}_{\tilde{R}} \equiv i\gamma_3\gamma_2, \hat{X}_{\tilde{R}} \equiv -i\gamma_2\gamma_1$ . Mapping the problem to that of a two spin 1/2, we can write the state  $|\psi\rangle$  in Eq. (3) as  $|\psi\rangle = \hat{A}|\uparrow_L\uparrow_R\rangle + \hat{B}|\uparrow_L\downarrow_R\rangle + \hat{C}|\downarrow_L\uparrow_R\rangle + \hat{D}|\downarrow_L\downarrow_R\rangle$ , where  $\hat{A} = A, \hat{B} = D, \hat{C} = B, \hat{D} = C$ , and  $|\uparrow_i\rangle, |\downarrow_i\rangle$  are the eigenstates of  $\hat{Z}_i$ . For the given  $A, B, C, D$ , the maximal violation of the CHSH inequalities in the new partitioning (maximal with respect of the choice of  $O_L, O_R$ , cf. Eq. (1)) is given by

$$\mathcal{C}_{564|132} = 2\sqrt{1 + 4|AC - DB|^2}, \quad (5)$$

where  $\mathcal{C}_{135|246} > 2$  signals non-local correlations. This is achieved unless  $AC - BD = 0$ . Measurements of CHSH inequalities following the partitionings depicted in panels (c) and (d) of Fig. 1 yield  $\mathcal{C}_{421|563} = 2\sqrt{1 + 4|AB - CD|^2}$  and  $\mathcal{C}_{641|352} = 2\sqrt{1 + |A^2 + C^2 + D^2 - B^2|^2}$ . The condition  $\mathcal{C}_{135|246} = \mathcal{C}_{136|245} = \mathcal{C}_{456|123} = \mathcal{C}_{124|356} = 2$  can never be fulfilled, i.e. CHSH correlations will be non-local in at least one of the four partitions considered in Fig. 1.

It is important at this point to make the following observation. The partitioning of the MBS into two sets naturally leads to the definition of operators satisfying spin-1/2 algebra for each set. Different partitionings entails different sets of spin operators. Such a construction of operators is not unique for MBS. It can be done for any quantum system whose state is spanned in a 4-dimensional space. Consider the case of two real, physical, spin-1/2 degrees of freedom, associated with  $L$  and  $R$  respectively, which are geographically separated. One may construct the corresponding sets of operators  $Z_i, X_i, Y_i$ , as is depicted in Fig. 1(a). We now would like to switch to another partitioning (e.g., the one depicted in Fig. 1(b)), involving  $\tilde{R}$  and  $\tilde{L}$  respectively. Trying to express the spin operators associated with this partitioning

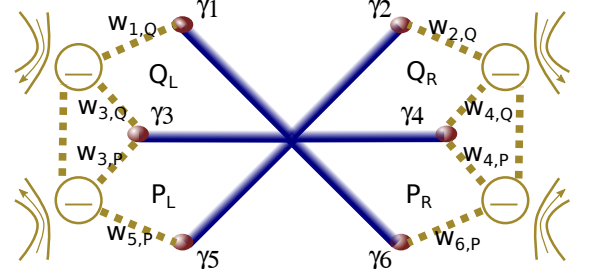


FIG. 2. Measurement of CHSH correlations in a Multi-terminal Majorana junction. The left and right measurement apparatus consist of quantum dots ( $Q_L, P_L, Q_R, P_R$ ) properly coupled to the Majorana end-states via tunnel coupling (dotted lines) of strength  $w_{\alpha,j}$ . The charge configuration of each dot is detected by a nearby charge sensor, schematically depicted as a quantum point contact. The measurement is performed by controlled time pulsed activations of the tunnel coupling  $w_{\alpha,j}$ .

in terms of the *real* spin operators, we have  $\hat{Z}_{\tilde{R}} = \hat{Z}_L$ , and  $\hat{Z}_{\tilde{L}} = \hat{Z}_R \otimes \hat{Z}_L$ . It then follows that  $Z_{\tilde{R}}$  and  $Z_{\tilde{L}}$  cannot be measured by two spatially separated detectors. This is in stark difference with the foregoing Majorana-based picture.

The statement that any state of the system violates the CHSH inequalities in at least one of the partitionings of Fig. 1 implies *finite* violation of CHSH inequalities. This is quantified by introducing the maximal value of CHSH correlations over the partitioning in Fig. 1,  $\mathcal{C}_0(|\psi\rangle) \equiv \max\{\mathcal{C}_{135|246}, \mathcal{C}_{564|132}, \mathcal{C}_{421|563}, \mathcal{C}_{641|352}\}$ . For any  $|\psi\rangle$ ,  $\mathcal{C}_0(|\psi\rangle) - 2$  is a positive finite quantity. There is therefore a minimum violation of the CHSH inequality over all states. From a standard minimization procedure over the parameters  $A, B, C, D$  [31], we obtain

$$\min_{|\psi\rangle} \{\mathcal{C}_0(|\psi\rangle)\} \approx 2.031. \quad (6)$$

Note that, since we restrict the analysis here to the four configurations of Fig. 1, the minimum value obtained is in fact a lower bound of the optimal minimum entanglement.

*Measurement* In order to implement the above ideas we need to measure operators of the form (1) and correlations thereof. While the emerging picture is quite general, we will demonstrate it by resorting to a specific measurement protocol: weakly tunnel-coupling quantum dots (QDs) to the multi-terminal Majorana junction [32, 33], and then measuring their charge. Let us describe the measurement procedure for operators associated with the  $L$  and  $R$  Majorana sets. We correspondingly define  $L$ - and  $R$ - detectors, each consisting of a double quantum dot tunnel-coupled to the three Majorana end-states in the set, as shown in Fig. 2. The coupling of the  $L$  detector

to the corresponding MBS is given by the Hamiltonian

$$H_{\text{det},L} = w_{3,Q}\gamma_3(c_{Q,L} - c_{Q,L}^\dagger) + w_{3,P}\gamma_3(c_{P,L} - c_{P,L}^\dagger) \\ + w_{1,Q}\gamma_1(c_{Q,L} - c_{Q,L}^\dagger) + w_{5,P}\gamma_5(c_{P,L} - c_{P,L}^\dagger), \quad (7)$$

where  $c_{j,L}$ ,  $j = Q, P$  are the electron destruction operators of each dot of the pair (all electrons are spin polarized) and  $w_{\alpha,j}$  are the tunneling matrix elements between the superconductor's end-points and the quantum dots. These dots are tuned such that only one orbital level per dot is relevant at the energy scales considered. The charge configuration of the double QD,  $(n_{Q,L}, n_{P,L})$ , with  $n_j = 0, 1$  can be detected by fast charge sensors, e.g. quantum point contacts [34–41]. The possibly time dependent tunnel coupling is controlled, e.g. by a nearby gate voltage [42]. One initially prepares the decoupled double QD in a generic superposition of singly occupied levels,  $|\phi_0\rangle = p_L|0, 1\rangle + q_L|1, 0\rangle$ , where  $|p_L|^2 + |q_L|^2 = 1$ . The tunnel coupling is then switched on for a finite time  $\Delta t$ , and is subsequently switched off. The state of the QDs may be modified, and the new charge configuration is read out by the charge sensors. Specifically we detect the probability,  $\mathcal{P}_{(1,0)}^L$  of finding the double dots in the configuration  $(1, 0)$ ,

While the strength and the duration of the QDs-Majorana coupling is adjustable, we consider here, for simplicity, the *weak measurement* limit. (Going beyond this limit is discussed below [31].) Expanding the time evolution,  $U = e^{-iH_{\text{det},L}\Delta t}$ , due to the system-detector coupling for small  $\Delta t$ , and setting for simplicity the initial state of the double QD to  $p_L = -iq_L = -i/\sqrt{2}$  and  $w_{\alpha,j} \in \mathbb{R}$ , the measured probability reads  $\mathcal{P}_{(1,0)}^L \approx 1/2 - (\eta_L - \lambda_L \langle \hat{O}_L \rangle) (\Delta t)^2$  to leading order in  $\eta_L = (|w_{1,Q}|^2 + |w_{3,Q}|^2 + |w_{3,P}|^2 + |w_{5,P}|^2)/2$ ,  $\lambda_L = (w_{1,Q}w_{3,P})^2 + (w_{3,Q}w_{5,P})^2 + (w_{1,Q}w_{5,P})^2$ . Here  $\hat{O}_L$  takes the form of Eq. (1) with  $\cos \theta_L = (w_{1,Q}w_{2,Q})/\sqrt{\lambda_L}$ ,  $\sin \theta_L \cos \phi_L = -\text{Re}(w_{2,Q}w_{3,P})/\sqrt{\lambda_L}$ ,  $\sin \theta_L \sin \phi_L = \text{Re}(w_{3,P}w_{1,Q})/\sqrt{\lambda_L}$ . This procedure constitutes a weak measurement of strength  $\lambda_L (\Delta t)^2$  of the operator  $\hat{O}_L$ . Tuning the parameters  $w_{i,j}$ ,  $i = 1, 3, 5$  and  $j = Q, P$  covers all operators of the local algebra of the left ( $L$ ) set. The same may be repeated to measure the observables represented by the operators  $\hat{O}_R$  of the right set, and the correlated measurements implied by the CHSH inequality are therefore executable. Specifically, referring to Fig. 2, one begins with the configuration  $p_L = p_R = -iq_L = -iq_R = -i/\sqrt{2}$ . Tunnel coupling the MBS to the QDs, and then sensing their final configuration, the probability to end-up in the  $(n_{Q,L} = 1, n_{P,L} = 0, n_{Q,R} = 1, n_{P,R} = 0)$  is

$$\mathcal{P}_{(1,0,1,0)} = \mathcal{P}_{(1,0)}^L \mathcal{P}_{(1,0)}^R + \frac{(\Delta t)^4}{6} (\eta_L^2 + \eta_R^2 + \lambda_L^2 + \lambda_R^2 \\ + 2\eta_L \lambda_L \langle O_L \rangle + 2\eta_R \lambda_R \langle O_R \rangle + \lambda_L \lambda_R \langle O_L O_R \rangle), \quad (8)$$

where  $\lambda_R = (w_{2,Q}w_{6,P})^2 + (w_{2,Q}w_{4,P})^2 + (w_{4,Q}w_{6,P})^2$  and  $\eta_R = (|w_{2,Q}|^2 + |w_{4,Q}|^2 + |w_{4,P}|^2 + |w_{6,P}|^2)/2$ . Eq.

(8) provides us with a way to evaluate the correlators of the type  $\langle O_L O_R \rangle$  (cf. Eq. (2)).

A few aspects of the measurement procedure are noteworthy. We first comment that the operators of the left and of the right set commute. It thus follows that they can be measured simultaneously; non-universal details of the time sequence concerning on-and-off switching of the tunneling matrix elements are immaterial. Second, the weak limit of the measurement offers a simple and immediate interpretation of the results, however the essence of the analysis remains unchanged at stronger system-detector interaction, although the calibration of the detector may become more involved. Finally, although the proposed measurement protocol is in principle feasible, it requires control of the individual tunnel matrix elements between the dots and the wires in order to measure different operators. This might present an experimental challenge. Other variants of the protocol may be better suited to experimental implementation. For example, the operators needed for this protocol may be designed by controlling individual QD's energy levels, or possibly by Majorana-to-charge conversion measurements [16].

*Conclusions* We have identified a minimal complexity MBS array: a junction with 6 segments delineating an 8-fold degenerate subspace defined by 6 Majorana end points. Unlike paradigmatic quantum states of two spin-1/2 particles that may (e.g. spin singlet) or may not (spin triplet-1) be entangled, we have shown that *any* state in the 4-dimensional fixed-parity degenerate space (e.g., odd parity) is *non-locally entangled*. This comes with a minimal bound on the violation of the CHSH inequality (Eq. (6)). We also presented a detector design, amenable to experimental implementation, and showed how to obtain CHSH correlation functions. Specifically, we discussed the limit of a weak measurement protocol. This ubiquitous non-locality, expressed through non-local entanglement, reflects the intrinsic property of MBS as carriers of fractionalized fermionic degree of freedom. Verification of non-local entanglement requires repeated measurements of CHSH correlations on replica of the same state, with at least 4 different partitioning (into  $L$  and  $R$  sets) of the Majorana degrees of freedom. The CHSH inequality will be broken for at least one of these partitioning. Measuring the operators associated with different partitionings may be achieved through tuning of the Majorana-QDs couplings, representing non-projective measurements. Interestingly, a recent work [43] has used the generation of entanglement to demonstrate how a newly designed gate may extend the possible set of operations with MBSs to form a framework for universal quantum computation [44]. Generalizations of the present analysis will involve  $2N > 6$  MBS junctions, as well as designs consisting of parafermions.

We acknowledge support from ISF grant 1349/14, DFG grant RO 2247/8-1, CRC 183 of the DFG, the IMOS Israel-Russia program, and the Minerva Founda-

tion.

- 
- [1] G. Moore and N. Read, Nucl. Phys. B **360**, 362 (1991).
  - [2] N. Read and D. Green, Phys. Rev. B **61**, 10267 (2000).
  - [3] A. Kitaev, Physics-Uspekhi **44**, 16 (2001).
  - [4] R. M. Lutchyn, J. D. Sau, and S. Das Sarma, Phys. Rev. Lett. **105**, 077001 (2010).
  - [5] Y. Oreg, G. Refael, and F. von Oppen, Phys. Rev. Lett. **105**, 177002 (2010).
  - [6] F. Wilczek, Nat. Phys. **5**, 614 (2009).
  - [7] F. Wilczek, Phys. Rev. Lett. **49**, 957 (1982).
  - [8] A. Stern, Nature **464**, 187 (2010).
  - [9] C. Nayak, S. H. Simon, A. Stern, M. Freedman, and S. Das Sarma, Rev. Mod. Phys. **80**, 1083 (2008).
  - [10] V. Mourik, K. Zuo, S. M. Frolov, S. R. Plissard, E. P. A. M. Bakkers, and L. P. Kouwenhoven, Science **336**, 1003 (2012).
  - [11] A. Das, Y. Ronen, Y. Most, Y. Oreg, M. Heiblum, and H. Shtrikman, Nat. Phys. **8**, 887 (2012).
  - [12] H. O. H. Churchill, V. Fatemi, K. Grove-Rasmussen, M. T. Deng, P. Caroff, H. Q. Xu, and C. M. Marcus, Phys. Rev. B **87**, 241401 (2013).
  - [13] S. Nadj-Perge, I. K. Drozdov, J. Li, H. Chen, S. Jeon, J. Seo, A. H. MacDonald, B. A. Bernevig, and A. Yazdani, Science **346**, 602 (2014).
  - [14] S. M. Albrecht, A. P. Higginbotham, M. Madsen, F. Kuemmeth, T. S. Jespersen, J. Nygård, P. Krogstrup, and C. M. Marcus, Nature **531**, 206 (2016).
  - [15] M. T. Deng, S. Vaitiekėnas, E. B. Hansen, J. Danon, M. Leijnse, K. Flensberg, J. Nygard, P. Krogstrup, C. M. Marcus, Science **354**, 1557 (2016).
  - [16] D. Aasen, M. Hell, V. Mishmash, A. Higginbotham, J. Danon, M. Leijnse, T. S. Jespersen, J. A. Folk, C. M. Marcus, K. Flensberg, et al., Phys. Rev. X **6**, 031016 (2016).
  - [17] S. Plugge, L. A. Landau, E. Sela, A. Altland, K. Flensberg, and R. Egger, Physical Review B, **94**, 174514 (2016).
  - [18] S. Plugge, A. Rasmussen, R. Egger, and K. Flensberg, New Journal of Physics **19**, (2017).
  - [19] L. Fu, Phys. Rev. Lett. **104**, 056402 (2010).
  - [20] K. Michaeli, L. A. Landau, E. Sela, and L. Fu, arXiv:1608.00581 (2016).
  - [21] S. Vijay, and L. Fu, Physical Review B **94**, 235446 (2016).
  - [22] B. Zocher, and B. Rosenow, Phys. Rev. Lett. **111**, 036802 (2013).
  - [23] S. Rubbert and A. R. Akhmerov, Phys. Rev. B **94**, 115430 (2016).
  - [24] Hereafter we refer to entanglement of spatially distinct degrees of freedom.
  - [25] J. Bell, Physics **1**, 195 (1965).
  - [26] M. Giustina, M. A. M. Versteegh, S. Wengerowsky, J. Handsteiner, A. Hochrainer, K. Phelan, F. Steinlechner, J. Kofler, J.-Å. Larsson, C. Abellán, et al., Phys. Rev. Lett. **115**, 250401 (2015).
  - [27] B. Hensen, H. Bernien, A. E. Dréau, A. Reiserer, N. Kalb, M. S. Blok, J. Ruitenbergh, R. F. L. Vermeulen, R. N. Schouten, C. Abellán, et al., Nature **526**, 682 (2015).
  - [28] J. F. Clauser, M. A. Horne, A. Shimony, and R. A. Holt, Phys. Rev. Lett. **23**, 880 (1969).
  - [29] J. Alicea, Y. Oreg, G. Refael, F. von Oppen, and M. P. a. Fisher, Nat. Phys. **7**, 412 (2011).
  - [30] B. S. Cirel'son, Lett. Math. Phys. **4**, 93 (1980).
  - [31] See supplementary material.
  - [32] K. Flensberg, Phys. Rev. Lett. **106**, 090503 (2011).
  - [33] M. Leijnse and K. Flensberg, Phys. Rev. Lett. **107**, 210502 (2011).
  - [34] M. Field, C. G. Smith, M. Pepper, D. A. Ritchie, J. E. F. Frost, G. A. C. Jones, and D. G. Hasko, Phys. Rev. Lett. **70**, 1311 (1993).
  - [35] J. M. Elzerman, R. Hanson, J. S. Greidanus, L. H. Willems van Beveren, S. De Franceschi, L. M. K. Vandersypen, S. Tarucha, and L. P. Kouwenhoven, Phys. Rev. B **67**, 161308 (2003).
  - [36] J. M. Elzerman, R. Hanson, L. H. Willems van Beveren, B. Witkamp, L. M. K. Vandersypen, and L. P. Kouwenhoven, Nature **430**, 431 (2004).
  - [37] J. R. Petta, A. C. Johnson, C. M. Marcus, M. P. Hanson, and A. C. Gossard, Phys. Rev. Lett. **93**, 186802 (2004).
  - [38] J. R. Petta, Science **309**, 2180 (2005).
  - [39] N. P. Oxtoby, H. M. Wiseman, and H.-B. Sun, Phys. Rev. B **74**, 045328 (2006).
  - [40] Z. Shi, C. B. Simmons, D. R. Ward, J. R. Prance, R. T. Mohr, T. S. Koh, J. K. Gamble, X. Wu, D. E. Savage, M. G. Lagally, et al., Phys. Rev. B **88**, 075416 (2013).
  - [41] D. R. Ward, D. Kim, D. E. Savage, M. G. Lagally, H. Foote, M. Friesen, S. N. Coppersmith, and M. A. Eriksson, Npj Quantum Information **2**, 16032 (2016).
  - [42] Note that we do not demand here a time-dependent control of the individual tunnel coupling matrix elements, but rather an overall on-and-off switching of the QDs-Majorana coupling. The relative strength of the tunnel couplings  $w_{j,k}$  can be fixed, e.g., at the fabrication stage.
  - [43] D. J. Clarke, J. D. Sau, and S. Das Sarma, Phys. Rev. X **6**, 021005 (2016).
  - [44] It has been shown in Ref. 43 that braiding operations on a 6-MBS setup will not be capable of producing entanglement in the computational basis. Our procedure employs a more general basis.

## SUPPLEMENTARY MATERIAL

### S1. MEASUREMENT PROTOCOL BEYOND THE WEAK LIMIT

In the manuscript we analyze the measurement protocol in the weak measurement regime. Specifically we consider there the probability for the transition of the detector's dots states from  $(|0, 1\rangle_L + |1, 0\rangle_L)/\sqrt{2} \otimes (|0, 1\rangle_R + |1, 0\rangle_R)/\sqrt{2}$  to  $|1, 0\rangle_L \otimes |1, 0\rangle_R$ . The transition probability is extracted by detecting the dots configuration  $(n_{Q,L}, n_{P,L}, n_{Q,R}, n_{P,R}) = (1, 0, 1, 0)$ . The weak measurement regime is obtained for small system-detector coupling and/or short measurement time. The transition probability is then dominated by the leading order term in  $(\Delta t)^4$ . This regime allows to conveniently relate the measured probabilities to the system's observables [Eq. (8)] entering the CHSH inequalities. Going beyond the weak measurement regime makes the relation to the system's observables more complicated, but it does not undermine the validity of the measurement protocol. Here we analyze the measurement signal for arbitrary parameters' strengths.

The analysis of the general-strength measurement can be formulated in terms of generalised positive operator valued measurements (POVM), which describe all possible outcomes of the charge configurations of the dots. The different outcomes of a charge measurement are then labelled by all possible combinations of  $n_j = 0, 1$ . The process can formally be described in terms of Kraus operators

$$M_{(n_{Q,L}, n_{P,L}, n_{Q,R}, n_{P,R})} = M_{L, (n_{Q,L}, n_{P,L})} \cdot M_{R, (n_{Q,R}, n_{P,R})}, \quad (S9)$$

$$M_{L, (n_{Q,L}, n_{P,L})} = \text{tr}_{\text{detL}} \{ |\Psi_{L, (n_{Q,L}, n_{P,L})}\rangle \langle \Psi_{L, (n_{Q,L}, n_{P,L})}| \}, \quad (S10)$$

$$M_{R, (n_{Q,R}, n_{P,R})} = \text{tr}_{\text{detR}} \{ |\Psi_{R, (n_{Q,R}, n_{P,R})}\rangle \langle \Psi_{R, (n_{Q,R}, n_{P,R})}| \}, \quad (S11)$$

$$\begin{aligned} |\Psi_{L, (n_{Q,L}, n_{P,L})}\rangle &= \left( c_{Q,L}^\dagger c_{Q,L} \right)^{n_{Q,L}} \left( c_{Q,L} c_{Q,L}^\dagger \right)^{1-n_{Q,L}} \left( c_{P,L}^\dagger c_{P,L} \right)^{n_{P,L}} \left( c_{P,L} c_{P,L}^\dagger \right)^{1-n_{P,L}} \\ &\quad \cdot \exp(-iH_{\text{det,L}}\Delta t) (Q_L c_{Q,L}^\dagger + p_L c_{P,L}^\dagger) |0\rangle_L, \\ |\Psi_{R, (n_{Q,R}, n_{P,R})}\rangle &= \left( c_{Q,R}^\dagger c_{Q,R} \right)^{n_{Q,R}} \left( c_{Q,R} c_{Q,R}^\dagger \right)^{1-n_{Q,R}} \left( c_{P,R}^\dagger c_{P,R} \right)^{n_{P,R}} \left( c_{P,R} c_{P,R}^\dagger \right)^{1-n_{P,R}} \\ &\quad \cdot \exp(-iH_{\text{det,R}}\Delta t) (q_R c_{Q,R}^\dagger + p_R c_{P,R}^\dagger) |0\rangle_R, \end{aligned} \quad (S12)$$

where  $|0\rangle_L$ ,  $|0\rangle_R$  are the state of empty left and right dots respectively, and  $\text{tr}_{\text{detL}}$ ,  $\text{tr}_{\text{detR}}$  denotes the trace over the degrees of freedoms of the left and right dots (detectors). The probability to obtain a specific outcome  $(n_{A,L}, n_{B,L}, n_{A,R}, n_{B,R})$  and the corresponding state after the measurement are given by

$$P_{(n_{Q,L}, n_{P,L}, n_{Q,R}, n_{P,R})} = \text{tr} \left\{ M_{(n_{Q,L}, n_{P,L}, n_{Q,R}, n_{P,R})} \rho M_{(n_{Q,L}, n_{P,L}, n_{Q,R}, n_{P,R})}^\dagger \right\}, \quad (S13)$$

$$\rho' = M_{(n_{Q,L}, n_{P,L}, n_{Q,R}, n_{P,R})} \rho M_{(n_{Q,L}, n_{P,L}, n_{Q,R}, n_{P,R})}^\dagger / P_{(n_{Q,L}, n_{P,L}, n_{Q,R}, n_{P,R})}. \quad (S14)$$

The signal we are interested in is determined by the Kraus operator  $M_{(1,0,1,0)}$ . The expression for  $M_{(1,0,1,0)}$  can be simplified considerably by noting that  $[H_{\text{det,L}}, H_{\text{det,R}}] = 0$ , and that the left and right dots are detected and prepared in states of identical parity. One can then express

$$|\Psi_{L, (1,0)}\rangle = \left( c_{Q,L}^\dagger c_{Q,L} \right) \sum_{m=0}^{\infty} \frac{(-\Delta t^2)^m}{(2m)!} H_{\text{det,L}}^{2m} (q_L c_{Q,L}^\dagger + p_L c_{P,L}^\dagger) |0\rangle_L, \quad (S15)$$

where  $H_{\text{det,L}}^2 = \eta_L - \lambda_L O_L i(c_{Q,L} c_{P,L}^\dagger - c_{P,L} c_{Q,L}^\dagger)$ , with the coefficients defined in the main text. The specific form of  $H - \text{det,L}^2$ , which involves a single operator, allows to evaluate the series in Eq. (S15), yielding

$$|\Psi_{L, (1,0)}\rangle = \left( c_{Q,L}^\dagger c_{Q,L} \right) \left( \eta_L(\Delta t) - \lambda_L(\Delta t) O_L i(c_{Q,L} c_{P,L}^\dagger - c_{P,L} c_{Q,L}^\dagger) \right) (q_L c_{Q,L}^\dagger + p_L c_{P,L}^\dagger) |0\rangle_L \quad (S16)$$

where the time functions  $\eta_L$  and  $\lambda_L$  are expressed by the series

$$\eta_L(t) = \sum_{p=0}^{\infty} \sum_{s=0}^p \left[ \frac{t^{4p}}{(4p)!} \frac{(2p)!}{(2s)!(2p-2s)!} \eta_L^{2p-2s} \lambda_L^{2s} - \frac{t^{4p+2}}{(4p+2)!} \frac{(2p+1)!}{(2s)!(2p+1-2s)!} \eta_L^{2p+1-2s} \lambda_L^{2s} \right], \quad (S17)$$

$$\lambda_L(t) = \sum_{p=0}^{\infty} \left[ -\frac{\lambda_L^{2p+1} t^{4p+2}}{(4p+2)!} + \sum_{s=0}^{p-1} \left[ \frac{t^{4p}}{(4p)!} \frac{(2p)! \eta_L^{2p-2s-1} \lambda_L^{2s+1}}{(2s+1)!(2p-2s-1)!} - \frac{t^{4p+2}}{(4p+2)!} \frac{(2p+1)! \eta_L^{2p-2s} \lambda_L^{2s+1}}{(2s+1)!(2p-2s)!} \right] \right]. \quad (S18)$$

This leads to the expression of the Kraus operator

$$M_{L,(1,0)} = q_L \eta_L(\Delta t) + i p_L \lambda_L(\Delta t) O_L. \quad (\text{S19})$$

The result for  $M_{R,(1,0)}$  is identical upon replacing  $L \rightarrow R$ . We can finally write the probabilities of interest as

$$P_{(1,0)}^L = |q_L|^2 \eta_L^2 + |p_L|^2 \lambda_L^2 + 2 \text{Im}(q_L p_L^*) \eta_L \lambda_L \langle O_L \rangle \quad (\text{S20})$$

$$P_{(1,0)}^R = |q_R|^2 \eta_R^2 + |p_R|^2 \lambda_R^2 + 2 \text{Im}(q_R p_R^*) \eta_R \lambda_R \langle O_L \rangle \quad (\text{S21})$$

$$\begin{aligned} P_{(1,0,1,0)} &= (\eta_L^2(\Delta t) |q_L|^2 + \lambda_L^2(\Delta t) |p_L|^2) (\eta_R^2(\Delta t) |q_R|^2 + \lambda_R^2(\Delta t) |p_R|^2) \\ &\quad + 2 \langle O_L \rangle \text{Im}(q_L p_L^*) \eta_L(\Delta t) \lambda_L(\Delta t) (\eta_R^2(\Delta t) |q_R|^2 + \lambda_R^2(\Delta t) |p_R|^2) \\ &\quad + 2 \langle O_R \rangle \text{Im}(q_R p_R^*) \eta_R(\Delta t) \lambda_R(\Delta t) (\eta_L^2(\Delta t) |q_L|^2 + \lambda_L^2(\Delta t) |p_L|^2) \\ &\quad - 4 \langle O_L O_R \rangle \eta_L(\Delta t) \eta_R(\Delta t) \lambda_L(\Delta t) \lambda_R(\Delta t) \text{Im}(q_R p_R^*) \text{Im}(q_L p_L^*) \end{aligned} \quad (\text{S22})$$

In the limit of small time  $\Delta t$  or small coupling  $\lambda_L$ , the above expressions reduce to the one in the manuscript, which correspond to the weak measurement regime. It is interesting to note that for long time and/or strong coupling, the measurement does not approach a strong projective measurement. This can be seen from Eq. (S19), which generically is not a projector (e.g.  $M_{L,(1,0)}^2 \neq M_{L,(1,0)}$ ). This feature is due to the finite dimension of the Hilbert space of the quantum dots used as an ancilla in the detection scheme. In this case the measurement time and coupling constants enter the Kraus operator through the superposition of a finite number of periodic functions. This fact can be seen explicitly from Eq. (S9), where  $\Delta t$  appears as a factor the exponential of a finite-dimensional matrix.

Importantly, Eq.(S22) shows that a measurement realized with the proposed scheme leads generically to a probability of the form Eq. (8) in the manuscript regardless of the duration and coupling strength. The proposed scheme can be therefore used as a test for CHSH inequalities even beyond the weak coupling limit. However, for intermediate measurement strength, the detector calibration requires a fine-tuning of the coupling time. This has to be compared with the weak measurement regime where a power of  $\Delta t$  appears as a common prefactor of the detector signal. Therefore, although the proposed measurement scheme works for arbitrarily strength of the measurements and coupling time, the weak measurement regime offers a more general form of the detector's signal, which, in turns, reduces the need for fine tuning in a given experimental setup.

## S2. CALCULATION OF THE MINIMAL VIOLATION OF THE CHSH INEQUALITY

In the manuscript we have introduced the minimal violation of CHSH inequalities,  $\mathcal{C} = \min_{|\psi\rangle} \{\mathcal{C}_0(|\psi\rangle)\} \approx 2.078$ , where  $\mathcal{C}_0(|\psi\rangle) \equiv \max \{\mathcal{C}_{135|246}(|\psi\rangle), \mathcal{C}_{564|132}(|\psi\rangle), \mathcal{C}_{421|563}(|\psi\rangle), \mathcal{C}_{641|352}(|\psi\rangle)\}$ . We report here the details of the calculation of  $\mathcal{C}$ .

Let us first introduce, for notational convenience,

$$C_1 \equiv 4|AD - BC|^2, C_5 \equiv 4|AC - BD|^2, C_4 \equiv 4|AB - CD|^2, C_6 \equiv |A^2 - B^2 + C^2 + D^2|^2.$$

We are looking for a state,  $|\psi_0\rangle$ , that will minimize  $\mathcal{C}_0$ , with the goal of showing that even the minimal value of  $\mathcal{C}_0$  exceeds the classical bound of CHSH inequalities. Since  $\mathcal{C}_{135|246} = 2\sqrt{1+C_1}$ ,  $\mathcal{C}_{564|132} = 2\sqrt{1+C_5}$ ,  $\mathcal{C}_{421|563} = 2\sqrt{1+C_4}$ ,  $\mathcal{C}_{641|352} = 2\sqrt{1+C_6}$ , depend monotonically on the newly defined quantities,  $|\psi_0\rangle$  is obtained by minimizing

$$\mathcal{K} = \min_{|\psi\rangle} \{\max \{C_1(|\psi\rangle), C_5(|\psi\rangle), C_4(|\psi\rangle), C_6(|\psi\rangle)\}\}.$$

We introduce also the convenient parametrization

$$A = a e^{i\alpha}, B = b e^{i\beta}, C = c e^{i\gamma}, D = d e^{i\delta}, \quad (\text{S23})$$

where  $a, b, c, d \in \mathbb{R}^+$ ,  $\alpha, \beta, \gamma, \delta \in [0, 2\pi)$ , and

$$a^2 + b^2 + c^2 + d^2 = 1. \quad (\text{S24})$$

A direct calculation shows that the stationary points of  $C_1$  with the constraint (S24) correspond to the global maximum,  $C_1 = 1$ , or the global minimum,  $C_1 = 0$ . The minimum  $C_1 = 0$  is obtained for the set of parameters where  $ad = bc$ , and  $\alpha + \delta - \gamma - \beta = 2n\pi$ . Repeating the search for extremal points of  $C_5$ ,  $C_4$ ,  $C_6$  yields similar sets

since the latter functions are all obtained from  $C_1$  by unitary transformations of the vector  $(A, B, C, D)^T$ . Since the intersection of all these sets of points is empty (i.e.  $C_1, C_5, C_4, C_6$  cannot be all simultaneously vanishing as stated in the manuscript), the state,  $|\psi_0\rangle$ , which minimizes  $\mathcal{K}$  must fulfil the condition  $C_i(|\psi_0\rangle) = C_j(|\psi_0\rangle)$ ,  $i \neq j$ .

A direct calculation shows that the stationary points of  $C_1$  with the conditions (S24) and

$$C_1 = C_5 \quad (\text{S25})$$

are the same global minima and maxima obtained without the constraint (S25). Iterating the argument for  $C_1 = C_5 = C_4$  one concludes that  $|\psi_0\rangle$  is constrained to the surface defined by

$$C_1 = C_5 = C_4 = C_6. \quad (\text{S26})$$

The minimum of  $C_1$  under the condition Eq. (S26) is not a global minimum. In fact, at most three of these functions can be simultaneously vanishing. Specifically, the set of points where  $C_1 = C_5 = C_4 = 0$  is

$$\{A = B = C = D\} \cup \{A = -C = B = -D\} \cup \{A = -B = C = -D\} \cup \{A = -B = D = -C\}$$

For all these points  $C_6 \neq 0$ .

In the following, to determine the minimum of  $C_1$  under the condition in (S26) and (S24), we first reparametrize the states constrained to  $C_1 = C_5 = C_4$ , and then impose the further condition  $C_1 = C_6$ . As a preliminary, starting from the parameters in Eq. (S23), we assume, without loss of generality,  $\delta = 0$ , since the latter can be reabsorbed in the overall (non-physical) phase of the state  $|\psi\rangle$ . We then have

$$C_1 = C_5 \implies (a^2 - b^2)(d^2 - c^2) = 4abcd \sin(\alpha - \beta) \sin(\gamma), \quad (\text{S27})$$

$$C_1 = C_4 \implies (a^2 - c^2)(d^2 - b^2) = 4abcd \sin(\alpha - \gamma) \sin(\beta), \quad (\text{S28})$$

$$C_5 = C_4 \implies (a^2 - d^2)(c^2 - b^2) = 4abcd \sin(\alpha) \sin(\beta - \gamma), \quad (\text{S29})$$

where the last equation is a redundant statement of the first two. To analyze the above constraints let us, as a first attempt, assume  $\sin(\alpha - \beta) \sin(\gamma) \neq 0$ ,  $\sin(\alpha - \gamma) \sin(\beta) \neq 0$ ,  $\sin(\alpha) \sin(\beta - \gamma) \neq 0$ ; the only solutions of the above equations are

$$a = b = c \neq d \quad (\text{S30})$$

$$a = b = d \neq c \quad (\text{S31})$$

$$b = c = d \neq a \quad (\text{S32})$$

$$a = c = d \neq b \quad (\text{S33})$$

Each of these equations, together with the normalization in Eq. (S24) allows us to eliminate three parameters. Each of these solutions (Eqs. (S30,S31,S32,S33)) implies

$$abcd \sin(\alpha - \beta) \sin(\gamma) = abcd \sin(\alpha - \gamma) \sin(\beta) = abcd \sin(\alpha) \sin(\beta - \gamma) = 0 \quad (\text{S34})$$

so either  $a = 0$ , or  $b = 0$ , or  $c = 0$ , or  $d = 0$ , or, contrary to our assumption,

$$\sin(\alpha - \beta) \sin(\gamma) = \sin(\alpha - \gamma) \sin(\beta) = \sin(\alpha) \sin(\beta - \gamma) = 0. \quad (\text{S35})$$

The condition  $a = 0$ , together with Eqs.(S26,S30,S31,S32,S33) necessarily leads to  $C_1 = C_5 = C_4 \neq C_6$ , and is therefore excluded. The same argument excludes  $b = 0, c = 0, d = 0$ . We thus need to abandon our earlier assumption. Eq. (S35), instead, has the different possible solutions:

$$\alpha = n\pi, \beta = m\pi, \gamma \in [0, 2\pi), \quad (\text{S36})$$

$$\alpha = n\pi, \gamma = m\pi, \beta \in [0, 2\pi), \quad (\text{S37})$$

$$\beta = n\pi, \gamma = m\pi, \alpha \in [0, 2\pi), \vee (\beta - \alpha = n\pi, \gamma - \alpha = m\pi, \alpha \in [0, 2\pi)), \quad (\text{S38})$$

where  $n, m \in \mathbb{Z}$ . As a result the surface defined by  $C_1 = C_5 = C_4$  consists of the combinations of each of Eqs. (S30,S31,S32,S33) with each of the Eqs. (S36,S37,S38).

Let us consider all these different cases separately. Using Eq. (S30) and Eq. (S38) in the definitions of  $C_1$  and  $C_6$  yields

$$C_{1,\pm} = 4a^2 \left( 1 - 2a^2 \pm 2a\sqrt{1 - 3a^2} \cos(\alpha) \right), \quad C_6 = |(1 - 3a^2) + a^2 e^{2i\alpha}|^2, \quad (\text{S39})$$



where  $C_1$  has two different expressions  $C_{1,\pm}$  corresponding to even and odd parities of  $m \cdot n$  respectively. Combining Eq. (S30) with Eq. (S36) yields

$$C_{1,\pm} = 4a^2 \left( 1 - 2a^2 \pm 2a\sqrt{1 - 3a^2} \cos(\gamma) \right), \quad C_6 = |(1 - 3a^2) + a^2 e^{2i\gamma}|^2, \quad (\text{S40})$$

and using Eq. (S30) and (S37) for  $C_1$  and  $C_6$  results in

$$C_{1,\pm} = 4a^2 \left( 1 - 2a^2 \pm 2a\sqrt{1 - 3a^2} \cos(\beta) \right), \quad C_6 = |(1 - a^2) - a^2 e^{2i\beta}|^2. \quad (\text{S41})$$

Combining Eq. (S31) and Eq. (S32) with each of the Eqs. (S36,S37,S38) leads to equations identical to (S39,S40,S41). Repeating the procedure for the case of Eq. (S33) results instead in different expressions for  $C_6$ . Specifically, combining Eq. (S33) with each of the Eqs. (S36,S37,S38) in the definition of  $C_1$  and  $C_6$  gives

$$C_{1,\pm} = 4a^2 \left( 1 - 2a^2 \pm 2a\sqrt{1 - 3a^2} \cos(\alpha) \right), \quad C_6 = |(5a^2 - 1) + a^2 e^{2i\alpha}|^2, \quad (\text{S42})$$

or

$$C_{1,\pm} = 4a^2 \left( 1 - 2a^2 \pm 2a\sqrt{1 - 3a^2} \cos(\gamma) \right), \quad C_6 = |(5a^2 - 1) + a^2 e^{2i\gamma}|^2, \quad (\text{S43})$$

or

$$C_{1,\pm} = 4a^2 \left( 1 - 2a^2 \pm 2a\sqrt{1 - 3a^2} \cos(\beta) \right), \quad C_6 = |(3a^2 - 1) + 3a^2 e^{2i\beta}|^2. \quad (\text{S44})$$

For each of the cases in Eqs. (S39,S40,S41,S42,S43,S44), we need to minimize  $C_1$  with  $C_1 = C_6$  and the further constraints  $0 \leq a \leq 1/\sqrt{3}$ ,  $\alpha, \beta, \gamma \in [0, 2\pi)$ . We are interested in the global minimum of  $C_1$  over all these different cases. Note that Eq.(S40) and Eq.(S39) are identical upon reparametrizing  $\gamma \rightarrow \alpha$ . The same holds for Eq.(S42) and Eq.(S43). Therefore we are left with the following eight minimization problems for  $C_{1\pm}$  over the parameters  $0 \leq a \leq 1/\sqrt{3}$  and  $\alpha, \beta, \gamma \in [0, 2\pi)$  with the condition  $C_1 = C_6$ :

$$C_{1,\pm} = 4a^2 \left( 1 - 2a^2 \pm 2a\sqrt{1 - 3a^2} \cos(\alpha) \right), \quad C_6 = |(1 - 3a^2) + a^2 e^{2i\alpha}|^2, \quad (\text{S45})$$

or

$$C_{1,\pm} = 4a^2 \left( 1 - 2a^2 \pm 2a\sqrt{1 - 3a^2} \cos(\beta) \right), \quad C_6 = |(1 - a^2) - a^2 e^{2i\beta}|^2, \quad (\text{S46})$$

or

$$C_{1,\pm} = 4a^2 \left( 1 - 2a^2 \pm 2a\sqrt{1 - 3a^2} \cos(\alpha) \right), \quad C_6 = |(5a^2 - 1) + a^2 e^{2i\alpha}|^2, \quad (\text{S47})$$

or

$$C_{1,\pm} = 4a^2 \left( 1 - 2a^2 \pm 2a\sqrt{1 - 3a^2} \cos(\beta) \right), \quad C_6 = |(3a^2 - 1) + 3a^2 e^{2i\beta}|^2. \quad (\text{S48})$$

From numerical calculations, we obtain for the lowest minimum in the above cases,  $\min_{a,\alpha} C_1 \approx 0.031$ , hence  $\mathcal{C} \approx 2.031$ .